Geostatistical Analysis of Pu-238 Contamination in Release Block D, Mound Plant, Miamisburg, Ohio

Sean A. McKenna

Sandia National Laboratories

Albuquerque, NM

Introduction

The Mound Plant in Miamisburg, Ohio, is a former DOE plutonium processing facility. The plant is now closed and site investigations and remedial action plans are in progress by DOE and contractors. Recently, site operators and regulators have become interested in a set of tools, based on geostatistical estimation and simulation techniques, to answer remediation and sample optimization questions. The purpose of this report is to document an example of the use of such techniques on a sub-site within the Mound plant. A brief overview of the principal concepts of geostatistics is given, followed by a discussion of geostatistics applied to the site at Mound. The results produced are discussed in an economic framework relative to future sampling and remediation. Results presented here are dependent on the assumptions stated in the text.

The site examined in this report is Release Block D. Within Release Block D, the concentrations of Pu-238 in soil, measured in pCi/g, are examined. Questions of concern to DOE within this release block are: 1)What areas of the site need to be remediated for a given action level?, 2) How much uncertainty is associated with the specification of remediation areas? 3) What are the remediation costs associated with different action levels as a function of the acceptable probability of failure and 4) If more samples are necessary, where are the best locations for them? This report attempts to answer these questions through the use of geostatistical simulation.

Geostatistics

Geostatistics is the study of data that exhibit spatial correlation. As many environmental and earth scientists have learned, samples of contaminants, sediments, porosity, etc. tend to be more similar when the samples are closely spaced and less similar as the distance between the sample locations increases. Geostatistics provides a means of quantifying this spatial correlation and also provides adaptations to classical regression techniques to take advantage of spatial correlation (Isaaks and Srivastava, 1989).

Variograms

At the heart of geostatistical analysis is the measurement and modeling of the degree and type of spatial correlation. These operations are generally accomplished through the calculation of an experimental variogram and then fitting of a model to that calculated variogram (Figure 1). The variogram is essentially a model of the increase in variability between sample locations as the distance (or time in Figure 1) between the samples increases. The variogram equation is given as:

$$\gamma(h) = \frac{1}{2n}\sum_{x=1}^{n}\left(Z(x) - Z(x+h)\right)^2 \quad .$$

The variogram equation is similar to the calculation of variance in classical statistics. In the calculation of variance, the mean is subtracted from each data point (each *Z(x)*), the differences are squared and then summed. In the variogram equation, the difference is taken between each data point and a data point a distance *h* away, the differences are squared and then summed. One-half of the average of these *n* differences for each separation distance is the variogram value, γ.

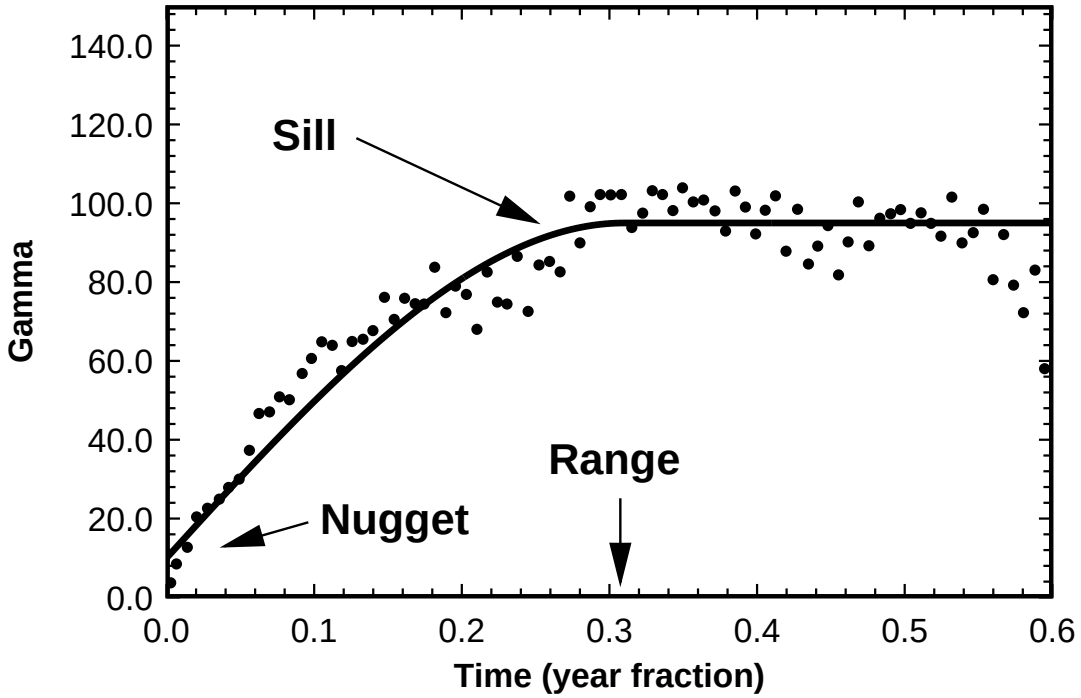

Figure 1. Example variogram defining the temporal correlation between daily closing values of the Standard and Poor's stock index over the 17 month period between 8/93 and 2/95. The range, sill and nugget are defined in the text.

There are several important features to a variogram model. As shown in Figure 1, the "range" is the distance at which the variogram model becomes parallel with the x-axis (Figure 1). The "sill" is the γ value at the range distance. Theoretically, the value of the sill, is equal to the variance of the data set. Intuitively, as the distance between sample locations decreases to zero, the amount of variability between samples should also decrease to zero. Often, variogram models do not go through the origin of the graph. In these cases, the variogram model y-intercept is known as the "nugget" value (Figure 1). The nugget effect generally represents a level of spatial variability occurring in the sample values below the smallest sample spacing as well as analytical errors.

The variogram model can be used to define spatial continuity for problems of estimation and simulation. Estimation is a linear interpolation technique, while simulation is a Monte-Carlo technique. Both techniques are used to assign property values to unsampled locations within the site domain.

Estimation and Simulation

Estimation techniques are used to derive an estimate of a concentration at an unsampled location(s). Estimation techniques commonly used in the earth sciences include inverse distance-

squared techniques, nearest neighbor polygons and kriging. All of these techniques can be classified as methods of interpolation, i.e., estimates of unknown concentrations at unsampled locations are derived by interpolating from known values at other locations. A simple example of estimation through interpolation is to hand an earth scientist a set of sample values along a transect and have the scientist estimate the values at all other locations. This exercise is usually completed by simply drawing a line to connect the available samples and estimating an expected value at any given location based on the connecting lines (Figure 2).

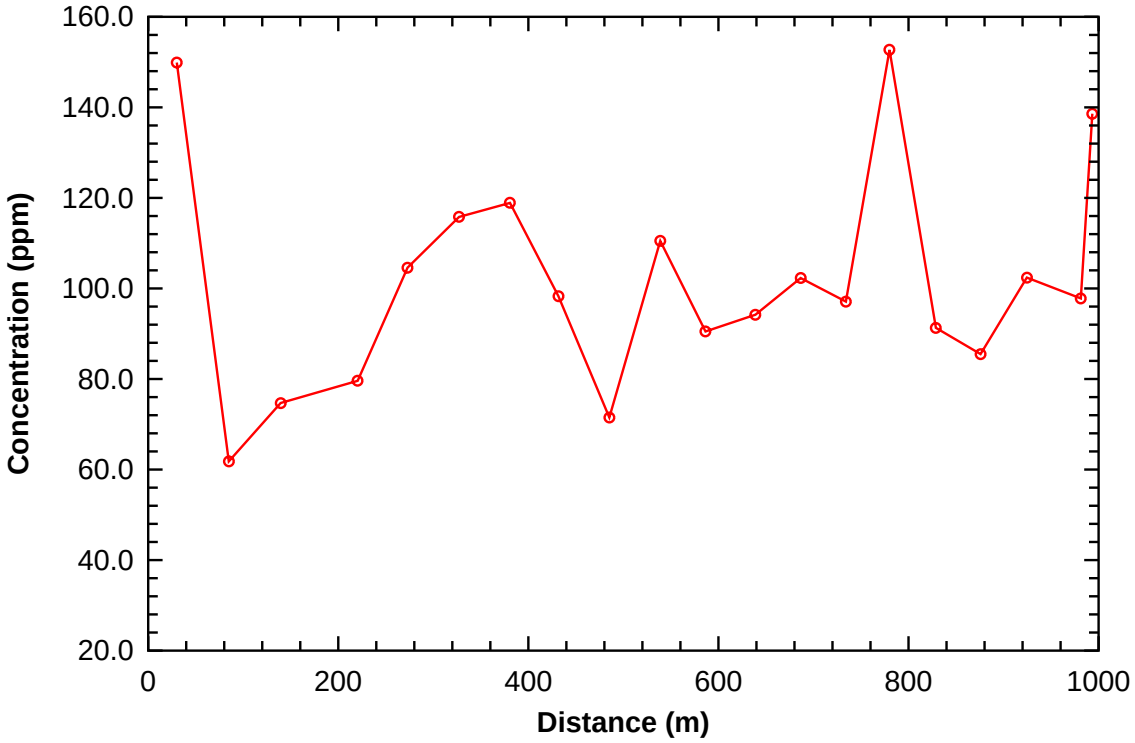

Figure 2. Example estimation of concentration values between 20 sample locations by a hand drawn interpolation. The horizontal lines correspond to the minimum and maximum sample values. The estimation is constrained within these values.

Of the three estimation techniques mentioned, only kriging exploits the model of spatial correlation derived through variogram modeling. Kriging is essentially the process of determining the expected value of concentration at a given location by calculating a weighted least-squares mean of other surrounding data points. The weights used in the least-squares estimation are calculated by using the model of spatial correlation as defined by the variogram. These weights account for the distance each data point is away from the location being estimated and the clustering of the data points (i.e., a number of points all close to each other provide redundant information concerning concentration at the point being estimated and are weighted less than a single point an equal distance away in another direction). Since kriging is an estimation technique, the concentration map derived from kriging will contain less variability than the actual sample data (lower variance). This smoothing effect will also ensure that the minimum and maximum of the esti-

mated map do not fall outside the bounds of the minimum and maximum of the sample data. A kriged estimate of concentration along the transect in Figure 2 would look very similar to the best guess drawn by hand.

The technique of simulation is designed to reproduce the measured level of variability in the sample data for each map of the concentration field. Whereas, estimation provides a single best guess of the concentration value at each location, simulation provides multiple possible maps of the concentration field, all of which honor the available data. Each equiprobable map of the contaminant distribution is known as a *realization*. An example of two simulations of concentration along the transect shown in Figure 2 are shown in Figure 3. Either one of these simulations could be the reality from which the samples were collected. Based on the limited samples available, it is not possible to determine what is the underlying reality. The multiple realizations of the concentration field created through geostatistical simulation are all equally probable depictions of reality based on the available data. The creation of many different possible maps of contamination at a site may seem to render the problem of creating a remediation map intractable compared to a single best guess map. However, multiple possible pictures of the contamination provide a means by which uncertainty in the contamination maps can be addressed. One interesting question that can be answered by examining multiple realizations of a contaminant field, is the probability of exceeding a specified concentration level at any location.

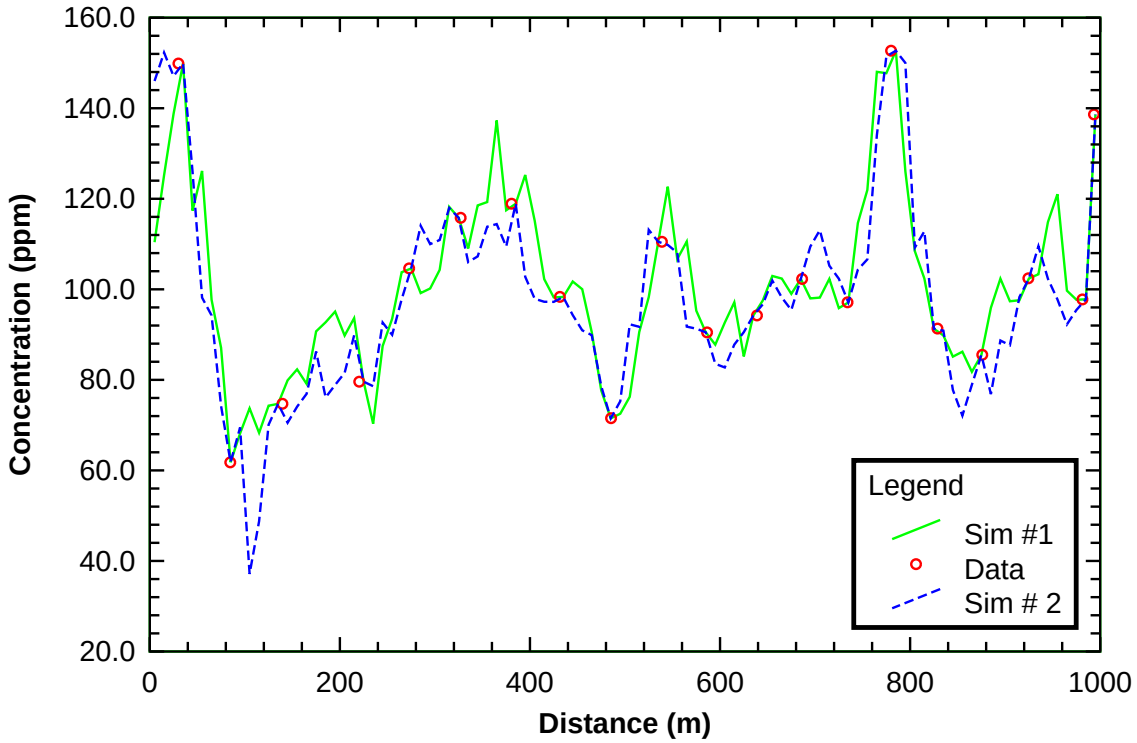

Figure 3. Two example simulations conditioned to the sample data. Note that the simulations contain more variability than the estimation and that simulated values are not constrained by the minimum and maximum sample concentrations.

Probability Mapping

Probability mapping is defined here as the use of geostatistical simulation to determine the probability of exceeding a specified level of a contaminant at each location in the simulation domain. For example, 100 realizations of a contaminant distribution can be created. If the action level is 25 pCi/g and 30 of the 100 realizations show concentrations greater than 25 at a given location, the probability of exceeding the action level at that location is 0.30, or 30%. This concept is shown in Figure 4. The mean value at each location is the estimate derived from kriging. Due to the spatial distribution of the samples and their concentration values, there may be locations in the same map with probabilities of exceeding 25 pCi/g from 0.0 to 1.0.

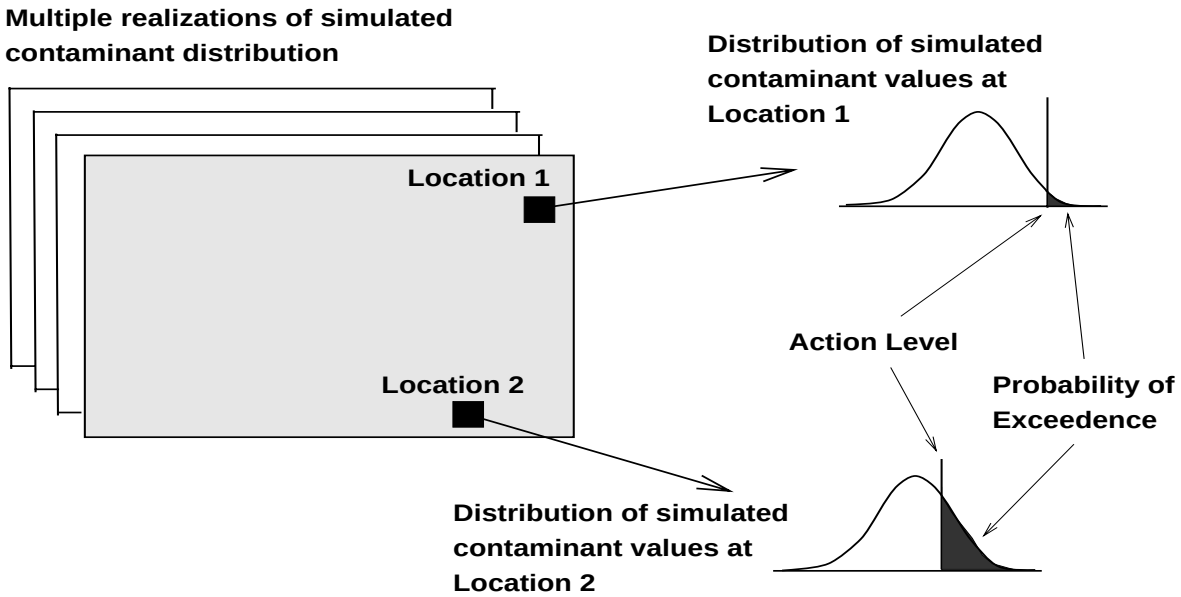

Figure 4. Conceptulaiztion of building a probability distribution at any spatial location through multiple geostatistical simulations. The probability of exceeding an action level at any location is simply the fraction of simulated concentrations across the ensemble of realizations that are greater than the action level.

Site Characterization and Data Set

Overview

The Release Block D site data were obtained from the appendices of a draft contractor report (EG&G, 1995). The site was sampled for Pu-238 and Th-232 on a square grid with 100 foot spacing. A map showing the sampling pattern and the extent of the domain examined in this study are shown in Figure 5. Note that there are several gaps in the sampling grid. Some of these are due to no sample recovery and some are due to information that is either missing or was not communicated to Sandia National Laboratories (SNL). The plutonium (Pu-238) data are analyzed in this study. The univariate distribution of the Release Block D plutonium data is shown in Figure 6 and the parameters describing the distribution are given in Table 1. Locations reported as having zero

concentration were set to 0.01 pCi/g to facilitate the normal-score transform in the geostatistical simulation process

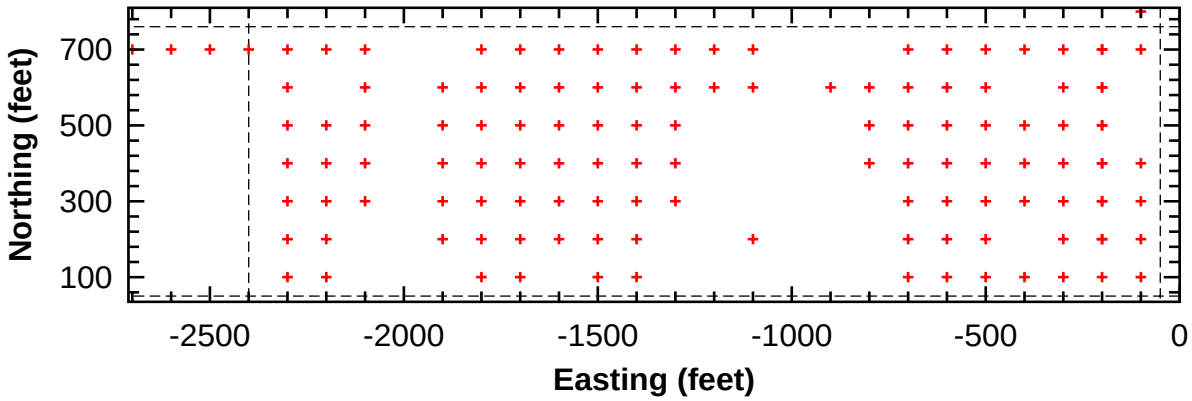

Figure 5. Map of the 127 sample locations in Release Block D used for variogram analysis. The geostatical simulations documented in this report were done on a subset of the map as denoted by the dashed lines. The bounding coordinates in feet for the geostatistical simulations are -2400 to -50 (easting), 50 to 760 (northing). This map uses the coordinate origin of the EG&G (1995) report. The positive westing coordinates reported in EG&G (1995) were converted to negative easting coordinates for this study.

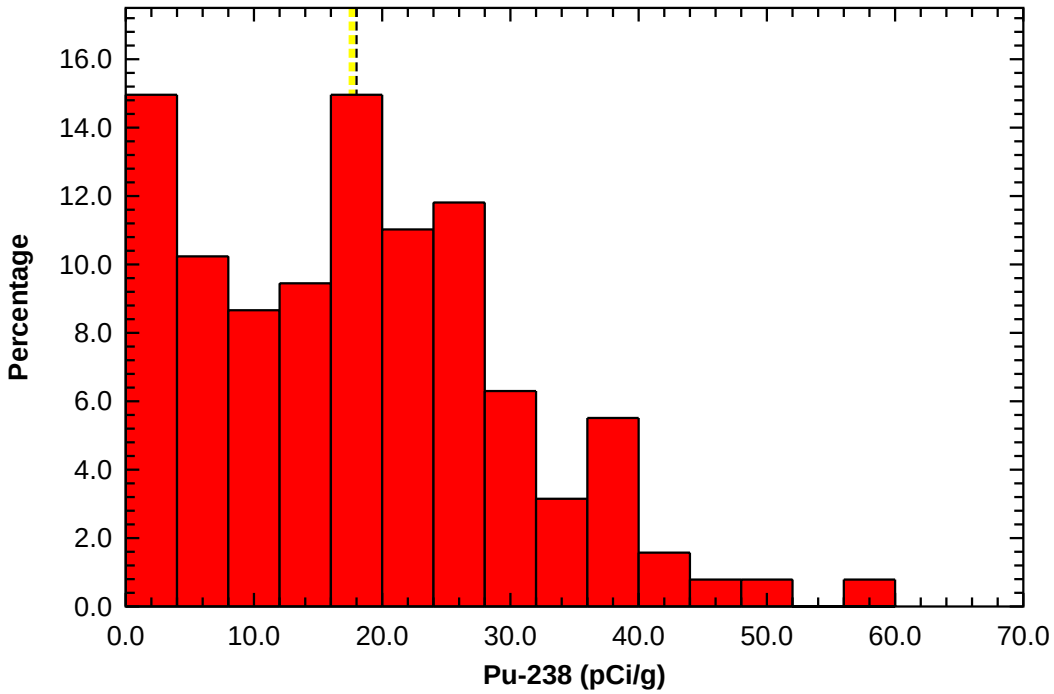

Figure 6. Histogram of the Pu-238 distribution of the 127 soil samples obtained on the PRS-379 site. The thick yellow and thin black dashed lines denote the mean and median of the distribution respectively.

Table 1: Distribution parameters for the sample data.

Parameter	Pu-238 pCi/g
Mean	17.52
Median	17.50
Standard Deviation	12.25
Coefficient of Variation	0.70
Minimum	0.01
Maximum	60.0
10th Percentile	1.0
90th Percentile	35.0
Number of Data	127

The concentrations within Release Block D were obtained with a field screening technique that has a reported lower detection limit of 25 pCi/g (D. Carfagno, pers. comm., 9/4/96). However, prior studies at the Mound site have shown the soil screening technique to provide good correlation with concentrations measured through geochemical analyses done in a laboratory at concentrations well below the 25 pCi/g detection limit (D. Carfagno, pers. comm., 9/4/96). The question arises as to what is the actual concentration below which the data are classified as non-detects? For this study, the assumption was made that any sample reporting a zero concentration is classified as a non-detect. This approach assumes that the concentrations below 25 pCi/g are reliable measurements and is consistent with communications from the Mound site.

Variography

In the practice of variogram calculation and modeling, a conceptual model defining the history of the physical or chemical property being analyzed is essential: "... it is subjective interpretation . . . that makes a good model; the data by themselves, are rarely enough" (Deutsch and Journel, 1992, p. 58). It is readily apparent that the data alone will not adequately define the variogram models at Release Block D. The main reason for this insufficiency of the data is the sample grid spacing of 100 feet, when, in fact, much of the spatial variability in Pu-238 at Release Block D occurs over distances less than 100 feet.

A complete conceptual model of how the Pu-238 was deposited across Release Block D has not been communicated to SNL. It is possible that a single mechanism or a number of mechanisms acted to deposit the Pu-238 across the site. In lieu of a well-defined conceptual model, two different conceptual models of contaminant deposition are considered during construction of the variograms for the Release Block D data: 1) "the random model" defines a process with a high degree of variability at short separation distances. This type of spatial distribution could result

from a spatially random process such as occasional spills of contaminant from a vehicle transporting the contaminant on various routes across the site. 2) “the continuous model” defines a deposition process that produces low variability in contaminant concentrations at short separation distances between samples. These type of deposits are generally created by a diffusive deposition process such as air fall from a smokestack. These two conceptual models are implemented in the variogram modeling by using different nugget values in the variogram models.

The simulation algorithm chosen to model the continuous distribution of contaminant concentrations is the multi-variate guassian algorithm coded into the program *sgsim* (Deutsch and Journel, 1992). This algorithm requires that the variogram be calculated in standard normal space. The standard normal distribution has a mean of zero and a standard deviation of 1.0 and is discussed thoroughly in almost any statistics textbook (e.g., Walpole and Myers, 1989). The mechanism for transforming the concentration data collected in the field to a standard normal distribution is the “normal-score” transformation. This transformation provides a robust means of transforming almost any distribution of data into a standard normal distribution. The normal score transformation is accomplished in this study using the program *nscore* (Deutsch and Journel, 1992).

The experimental normal-score variogram and the model fit to it representing the random conceptual model of contaminant emplacement are shown in Figure 7a. The parameters defining the model fit to the experimental variogram are given in Table 2. The model fit to the experimental variogram for the continuous deposition conceptual model is shown in Figure 7b and the model parameters are also given in Table 2. A double-nested structure was used to fit the variogram for the continuous deposition conceptual model. Calculation and modeling of the variograms was accomplished using the *vario* and *variofit* software packages in UNCERT (Wingle, et al., 1995)

Table 2: Variogram model parameters.

Deposition Model	Nest	Variogram Model Type	Nugget $(pCi/g)^2$	Sill $(pCi/g)^2$	Range (feet)
Random	1	Spherical	0.54	0.46	425.0
Continuous	1	Spherical	0.0	0.60	125.0
	2	Spherical		0.40	475.0

Simulation

The Release Block D site was discretized into 10x10 foot grid elements for the geostatistical simulations. Given the dimensions of Release Block D, this grid spacing allows for a total of 16,380 simulation elements (234x70). The extent of the simulation domain is described in the caption of Figure 5. It is noted that the simulations will replicate the distribution of the data across the site. Because of this conditioning to the univariate data distribution, the simulations will represent samples of concentration at the same scale as the samples collected in the field. This is conceptualized as a sample located at every grid centroid separated from every other sample by 10 feet of space in each direction. It is important to keep in mind that each simulated point does <u>not</u> represent the concentration across the 10x10 foot panel unless those samples were collected as composites within the 10x10 foot cells. The two normal-score variograms are used to create two ensembles of 100 concentration realizations each. The maximum possible simulated

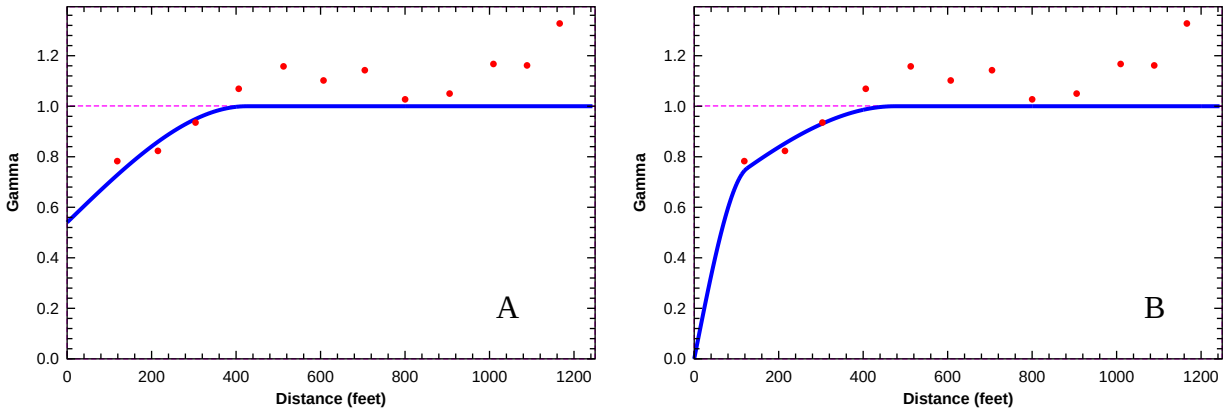

Figure 7. Modeled normal-score variograms for the random (A) and the continuous (B) conceptual models of contaminant deposition.

concentration value was set to be 100 pCi/g in all realizations. Example realizations created with the random and continuous conceptual models of deposition are shown in Figures 8 and 9.

All six of the realizations shown in Figures 8 and 9 have similar features. Low concentrations predominate between easting coordinates of -500 and -1100 and to the west of the -2000 easting coordinate. The highest concentration values occur along the southern edge of the of the domain near the -300 easting coordinate and also between easting coordinates of -1500 and -2000. The similarities between simulations are controlled by conditioning each simulation to the sample data. In areas without conditioning data, there can be large differences in the concentration maps between realizations. A clear example of this effect is the difference in concentration surrounding the -1050, 400 coordinates between realizations 50 and 75 on Figure 8.

The obvious difference between the simulations created with the random deposition model and the continuous deposition model is the smoothness of the images. The random deposition model creates simulations with a random “salt-and-pepper” appearance. These features of the image are controlled by the large nugget effect in the variogram. The large amount of variability in simulated concentrations separated by only 4 or 5 grid blocks is caused by the nugget effect. The long range correlation of the variogram produces areas of a similar range of concentrations near to each other. For the simulations created with the continuous model of deposition, there is a much smoother transition from a high value, through the full range of simulated values to a lower value.

The simulations can be processed to determine the total amount of predicted contaminant across the site. This calculation is accomplished by assuming that each measurement of concentration is representative of a 10’x 10’ x 0.5’ volumes of soil (as would be the case with composite sampling). Consequently, the simulated concentrations are also representative of the same volume of soil. The contaminant is assumed to be evenly distributed throughout the volume, and the soil is assumed to have a density of 100lbs/ft^3. Thisl calculation yields the amount of Pu-238 within the simulated domain in curies. The total simulated amount of curies within Release Block D are shown in Figure 10 as a function of the simulation number for both conceptual models of deposition. Because the same vector of random seed values was used in *sgsim* to create both ensembles of realizations, the general shape of the graphs is similar. However, for each pair of realizations, the total amount of curies is higher in the random deposition model compared to the

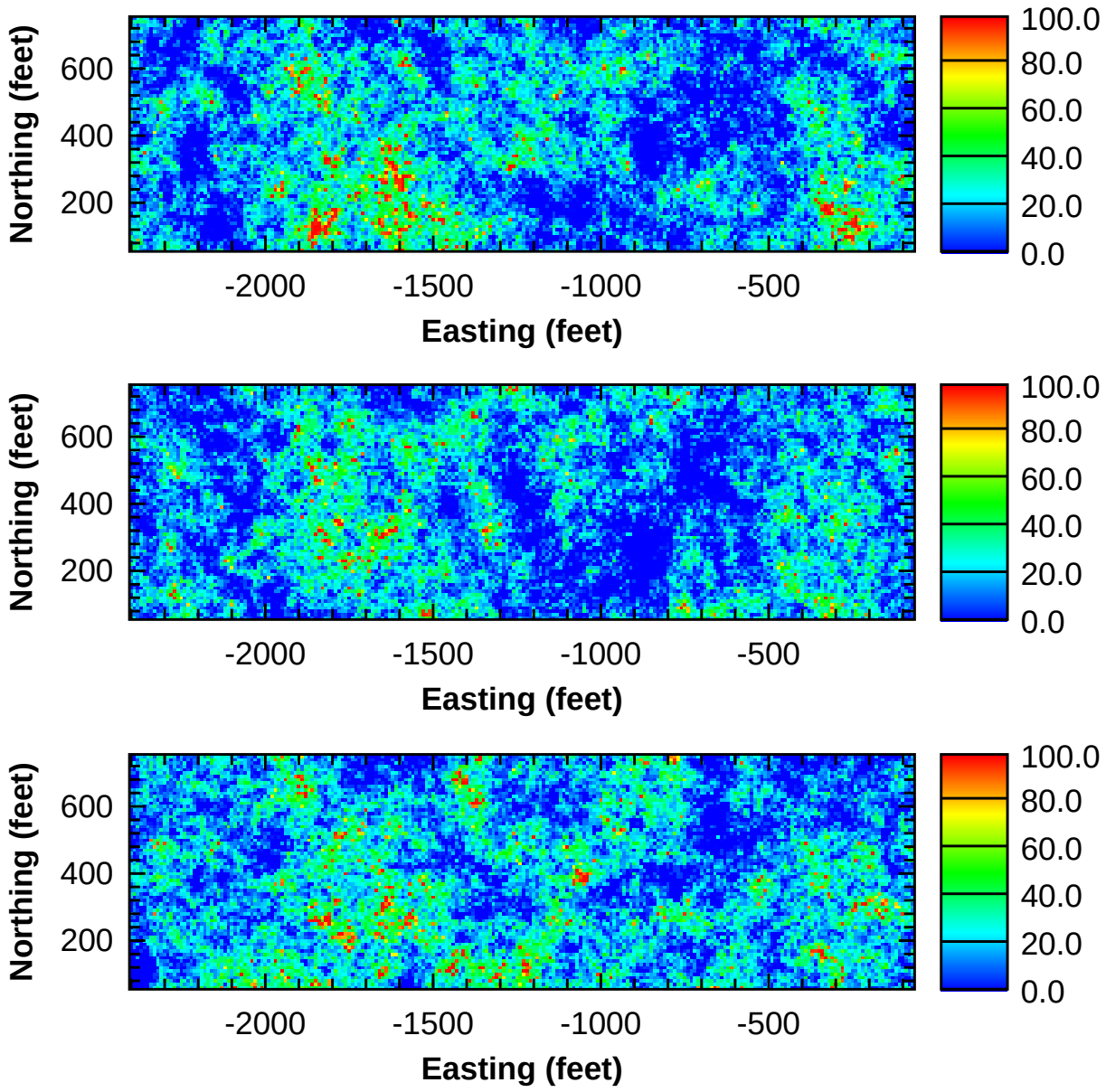

Figure 8. Three example realizations created with the random deposition conceptual model. The top image is realization #25, the center image is #50 and the bottom image is #75.

continuous deposition model. From Figure 10, the lowest and highest amount of total simulated concentration across the site for the random deposition model are given by realizations 59 and 75 respectively. For the continuous model of deposition, the lowest total amount of Pu-238 occurs in realization 63 and the highest amount in realization 76. Figures 11 and 12 show the low and high (best and worst case) realizations for each conceptual model of deposition.

One question that must be considered is whether or not 100 realizations are enough to capture the full variability of the concentration values and ensure the correct remediation decision at any

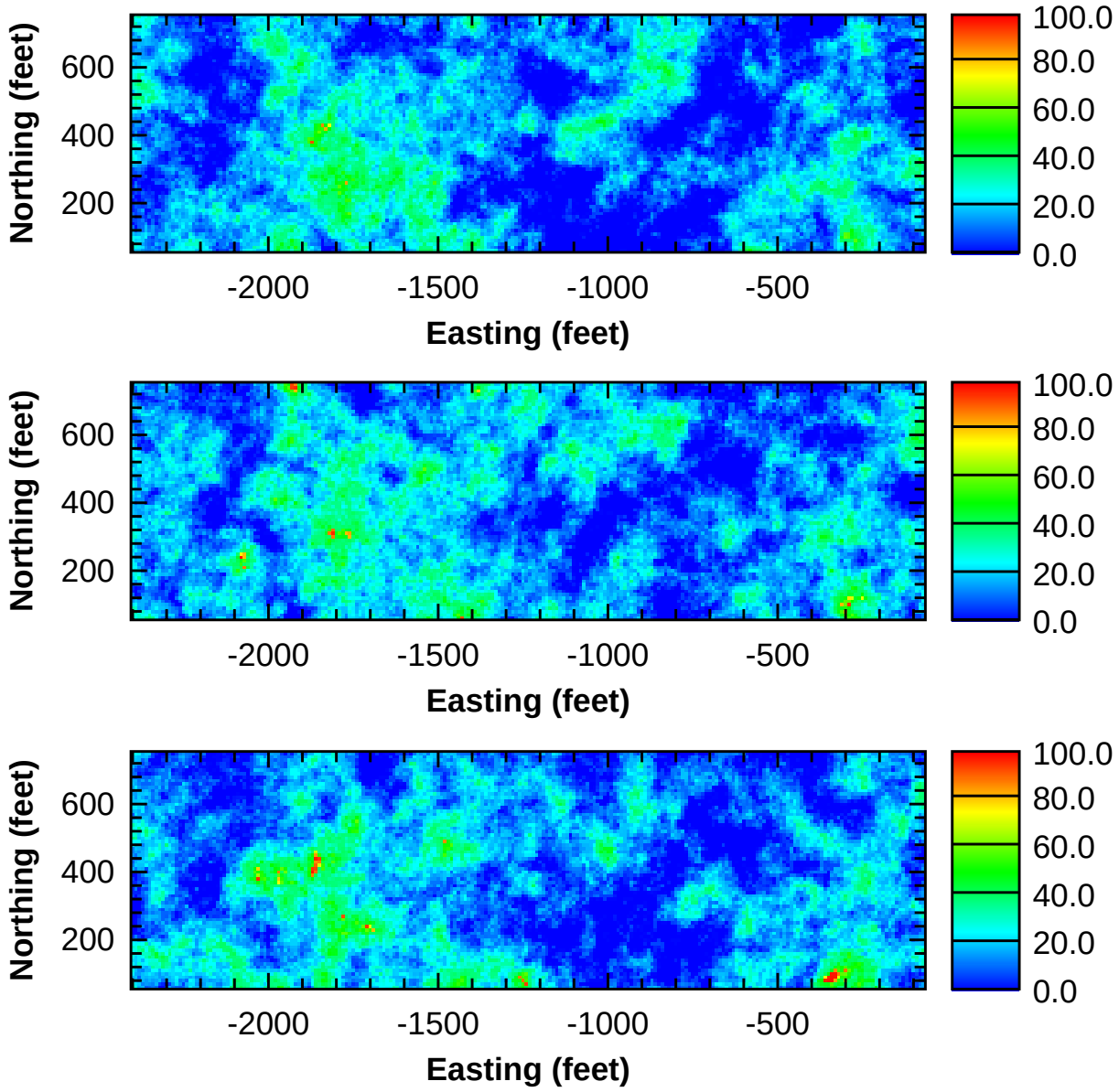

Figure 9. Three example realizations created with the continuous deposition conceptual model. The top image is realization #25, the center image is #50 and the bottom image is #75.

location. The concept of a representative elementary volume (REV) is taken from the ground water hydrology literature (Bear, 1972) to address this question. In the field of ground water hydrology, an REV is a volume of the porous media that is large enough to average out any discrete local effects of heterogeneity in the media, but small enough to not be affected by deterministic trends in the distribution of the property. A classic example of an REV is given by measuring porosity in a sandstone with a larger and larger sampler. At the smallest sample size the porosity will be either 0.0 or 1.0 depending on whether or not the sampler encounters a sand grain or a void space. As the size of the sample increases, the fluctuations in the porosity value will diminish as

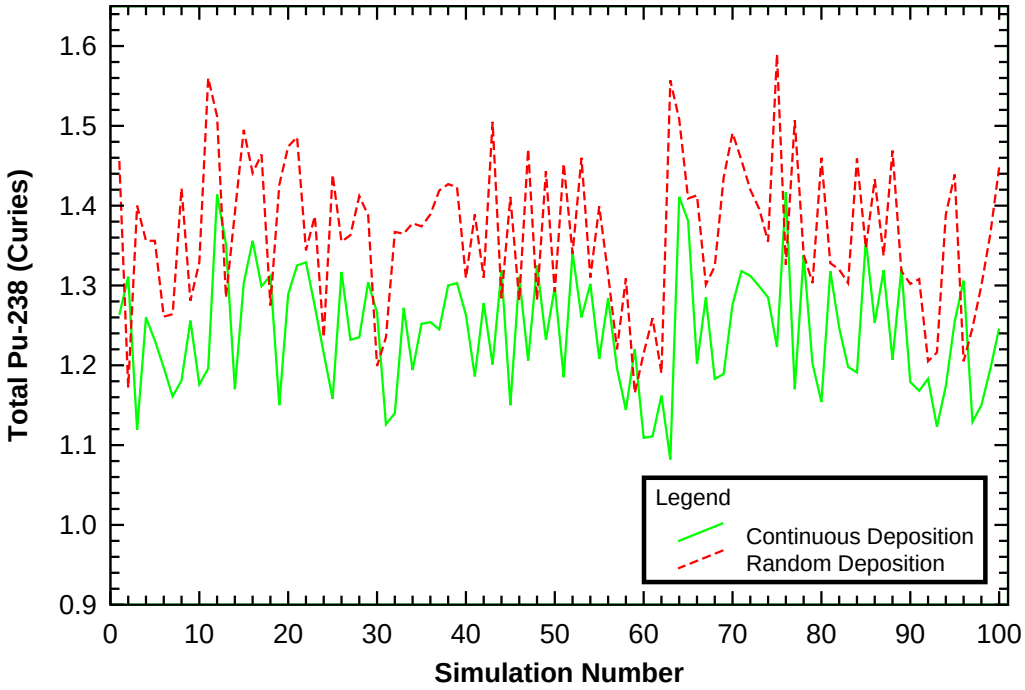

Figure 10. The total amount of contaminant on the site as a function of the simulation number for both conceptual models of deposition.

the sampler begins to sample a *representative* volume of the porous media. If the size of the sample continues to increase, portions of the sample will begin to come from other sedimentary units (e.g., a nearby shale) and the sampled value of the porosity will deviate from the representative value.

The REV concept can be applied to analyzing geostatistical simulations by recalling that at the basis of geostatistics, the ergodic hypothesis allows for the replacement of a spatially infinite sample by a *large* number of spatially finite, stochastically generated images. While this hypothesis is a basic tenet of geostatistics, the practical question of "What is *large*?" or at least l*arge enough* remains to be answered for the Pu-238 contamination at within Release Block D. In order to answer this question, the spatial averaging of the REV in ground water hydrology is replaced by a running average of concentration, across an ever increasing number of realizations. The calculated statistic is no longer an REV, but is now termed the *representative number of relizations* (RNR). If the average value stabilizes to a constant, representative value, then the number of realizations is deemed to be large enough.

The RNR is calculated at four different locations for each ensemble of realizations. The locations are chosen with respect to the conditioning data to cover the range of possible outcomes: a location with a generally high simulated concentration ("Location 1" at -1800, 250), a location with a generally low simulated concentration ("Location 2" at -650, 550), a location midway between relatively high and low concentration conditioning data ("Location 3" at -350, 100) and a location with a high kriging variance, as distant as possible from any conditioning data ("Location

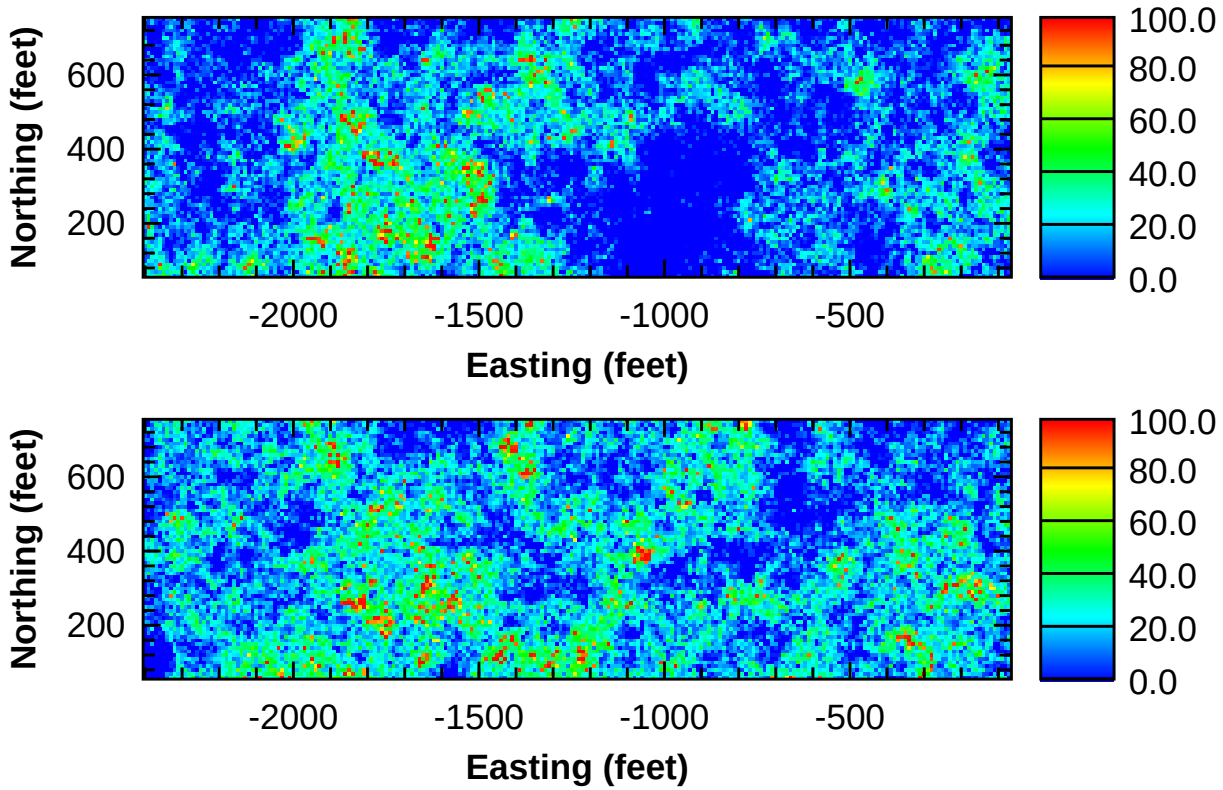

Figure 11. The best case (lowest total amount of curies) simulation (top) and the worst case (highest total amount of curies) simulation (bottom) for the random deposition conceptual model.

4" at -1050, 400). The values of the RNR are given in Figures 13 and 14 as a function of the number of simulations for the random and continuous conceptual models respectively.

The two graphs of the RNR's as a function of the number of simulations used in the averaging show that the average values at each of the four locations examined stabilize at approximately 90 simulations or less. The variability of the RNR calculated with the continuous deposition conceptual model is much lower than the RNR's created with the random deposition conceptual model. As expected, the RNR calculated at location 3, midway between a high and a low concnetration conditioning point has the highest variability. There do not appear to be any significant differences in the shape of the RNR graphs, other than the relative position on the Y-axes, between the four locations examined. Based on these RNR calculations, it is concluded that 100 simulations are enough for the probabilistic study of Pu-238 contamination within Release Block D.

Probability Mapping

Both ensembles of 100 realizations can be processed to create probability of exceedence maps. Three action levels were chosen and employed in the probability mapping: 10, 25 and 50 pCi/g. The 25 pCi/g action level corresponds to the ALARA goal set for the Mound facility. Higher action levels of 75 and 150 pCi/g employed at other locations across the Mound site would be of little use in Release Block D due to the measured data maximum of 60 pCi/g. The probability maps corresponding to the three action levels are displayed for the random and continuous models of deposition in Figures 15 and 16 respectively.

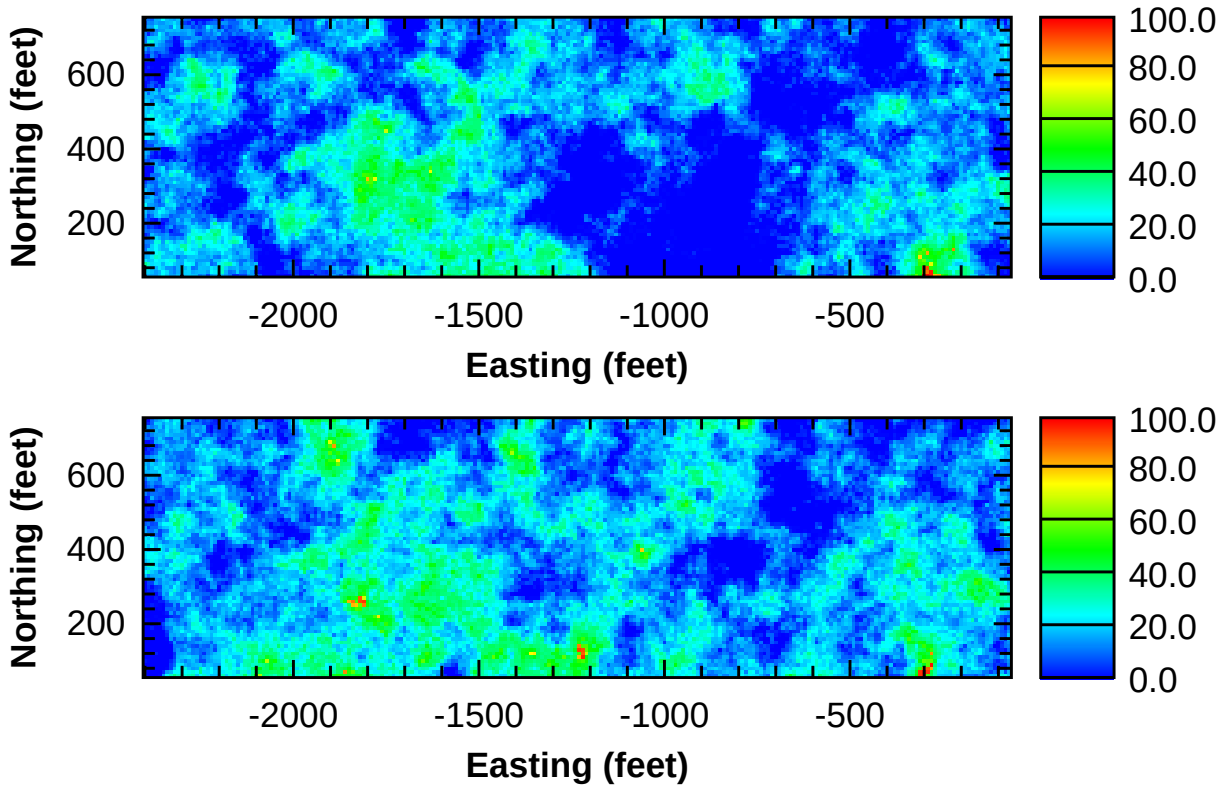

Figure 12. The best case (lowest total amount of curies) simulation (top) and the worst case (highest total amount of curies) simulation (bottom) for the continuous deposition conceptual model

The sample locations are apparent in the probability maps, especially the probability maps constructed with the random conceptual model of deposition. Since the simulations are conditioned to the available data, the sample locations can only have a probability of exceedence equal to 0.0 or 1.0. The simulated values at the data locations do not change from realization to realization, i.e., the actual sample value is returned in every simulation. If the sample value is below the action level, the probability of exceedence is 0.0; if the sample value is above the action level, the probability of exceedence is 1.0.

A probability map is further processed to develop a remediation map by selecting an acceptable probability of remediation failure (*pfail*) and then remediating all locations with a probability of failure greater than *pfail*. Example remediation maps for pfail = 0.05 at an action level of 25 pCi/g are shown in Figure 17. It is noted that in the case of an action level in the upper tail of the data distribution and a low *pfail*, the number of false negatives (leaving behind contaminated soil) can be well controlled. However, for this situation, the number of false positives (remediating locations that are clean) can become quite large.

The probability maps are used to generate plots of cost as a function of the probability of leaving behind a contaminated panel during the remediation (probability of failure in the remediation). These curves are predicated on the realization that cost-effective remediation can only be achieved if some probability of failure is accepted by the regulatory body. If the regulatory body is extremely risk averse, then the only solution may be to remediate the entire site. The cost curves present an effective way to display the relationship between cost and probability of reme-

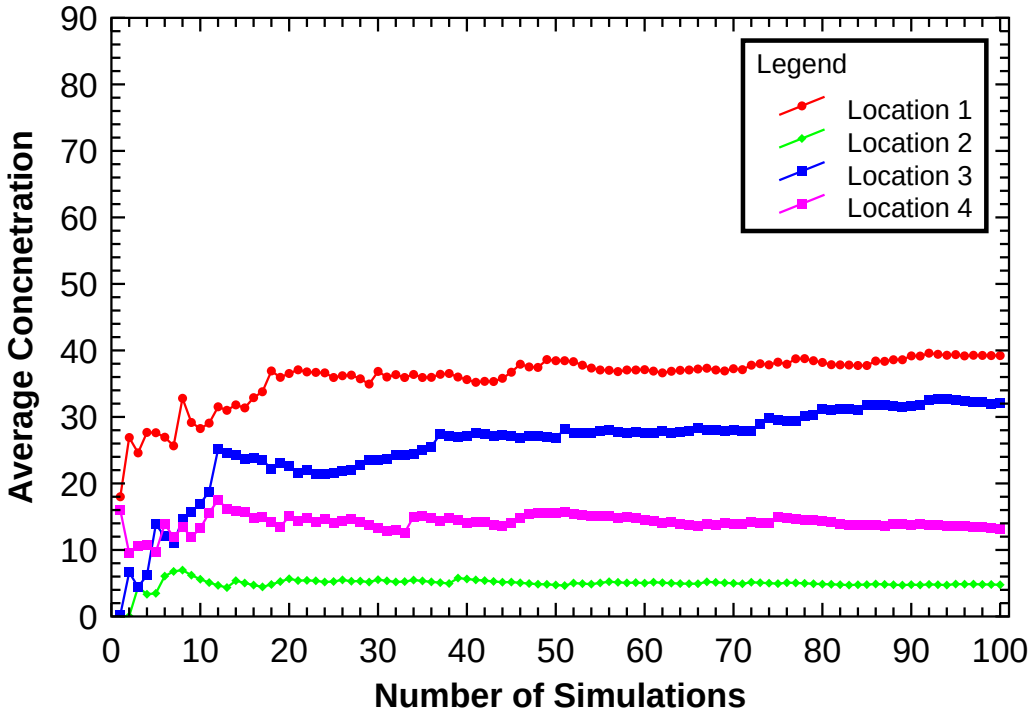

Figure 13. Representative number of realization (RNR) calculations for the concentrations at four locations. These graphs were constructed using the one-hundred simulations created with the random deposition conceptual model.

dial failure. These curves can also provide a focal point for discussion between the site owners, regulators and stakeholders concerning action levels and costs associated with various future land-use scenarios.

The probability maps shown in Figures 15 and 16 for the three action levels are used to develop cost curves for Release Block D. A key assumption made in calculating these cost curves is that the distribution and variograms of the sample data describe the spatial distribution of the Pu-238 for 10' x 10' by 0.5' remediation panels across the site. This assumption is that of composite sampling in the remediation panel at each sample location. The remediation cost is assumed to be $\$500.00/yd^3$. This cost figure is based on remediation costs documented at other locations within the Mound facility (EG&G, 1996). The resulting cost curves for Release Block D are shown in Figure 18.

For probabilities of failure less than 0.45, Figure 18 shows that the continuous deposition model is always the model with the lower remediation cost. The differences between the two models of deposition are greatest for the 50 pCi/g action level at low (< 0.05) probabilities of failure. This is expected due to the proximity of the 50 pCi/g action level to the tail of the data distribution. The cost curves in Figure 18 point out the tremendous difference in cost for the various action levels considered. At a five percent probability of failure, the differences in cost between the 25 pCi/g and the 50 pCi/g action levels are approximately 10.5 million dollars for the random deposition model results and 12.5 million dollars for the continuous deposition model results.

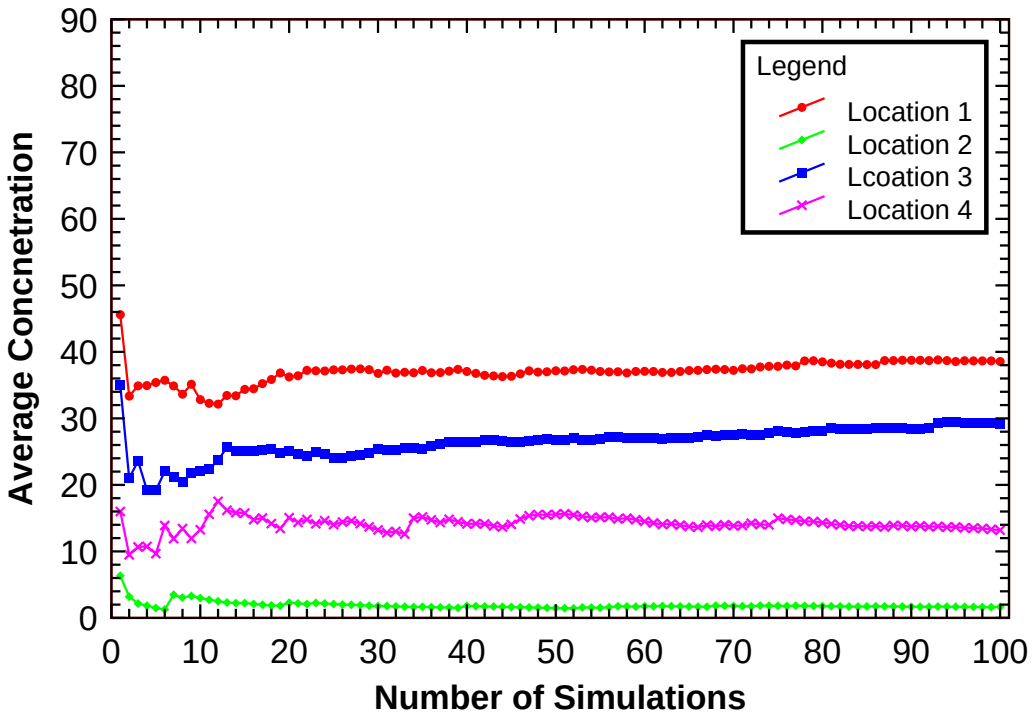

Figure 14. Representative number of realization (RNR) calculations for the concentrations at four locations. These graphs were constructed using the one-hundred simulations created with the continuous deposition conceptual model.

Follow-Up Sampling

Prior to finalizing a remediation plan, it is often prudent to acquire additional samples to augment the existing data. The placement of these samples should be optimized such that the information concerning a remediation decision is maximized. A number of techniques that have been proposed for optimal location of future samples (Burgess, et al., 1981; Englund and Heravi, 1994; Kyriakidis, 1996) with reduction of kriging variance being the most popular (see Barnes, 1989 and Olea, 1984 for a review of kriging variances as a means of sample optimization). In the past few years, decision-based sample optimization has proven to be superior to kriging variance for locating in-fill samples. This result is not surprising given that kriging variance is based solely on the data locations, not on the data values. By incorporating the data values of the initial sampling into the optimization through consideration of the action level, the amount of information gained by the additional samples can be maximized.

Several techniques have been proposed for incorporating the action level into optimizing the placement of additional samples. The first technique is an intuitive approach suggested by Rautman et al. (1994) that is simply targeting the locations with median probability of exceeding the action level (probabilities near 0.5). This approach is termed the “median probability” (MP) technique. The second approach involves targeting the locations with median probability of exceedence and also accounting for the variability between simulations at those locations. One variant of this approach is implemented in the OPTMAS program (Knowlton, et al., 1995) where

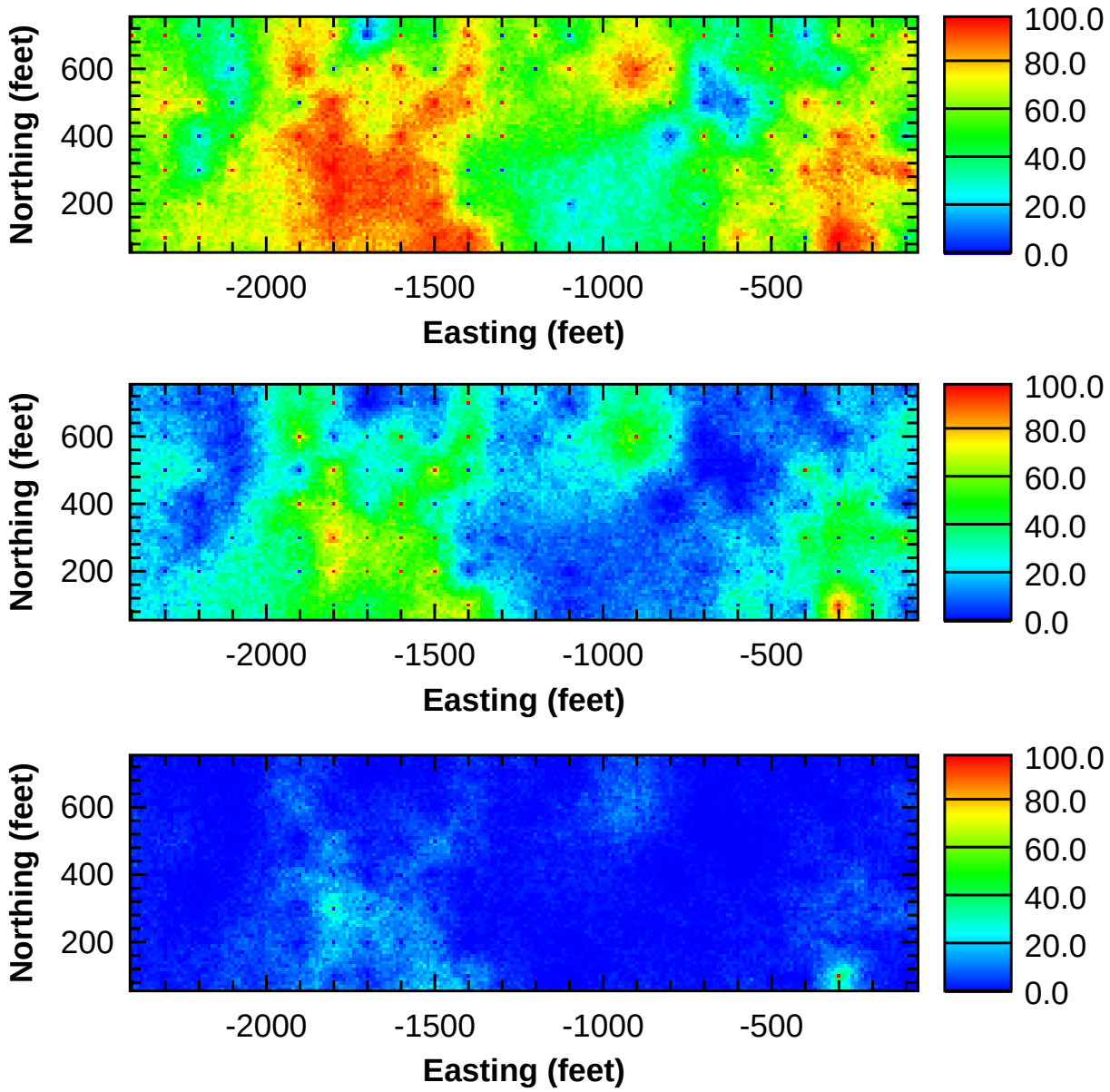

Figure 15. Probability of exceeding the action level (in percent) based on 100 realizations created with the random deposition conceptual model. The images correspond to action levels of 10 (top), 25 (center) and 50 (bottom) pCi/g.

a single additional sample is located along the median probability of exceedence contour line at the location of the highest simulation standard deviation. An extension of this approach is suggested here and is denoted as the “weighted standard deviation” (WSD) technique. The simulation standard deviation at any location is multiplied by a weight between 0.0 and 1.0. The weight is a function of the probability of exceeding the action level. For locations with a probability of exceedence equal to 0.5, the weight is 1.0. The value of the weight tails off to 0.0 as the probability of failure approaches both 0.0 and 1.0. The weighting function is shown schematically in Fig-

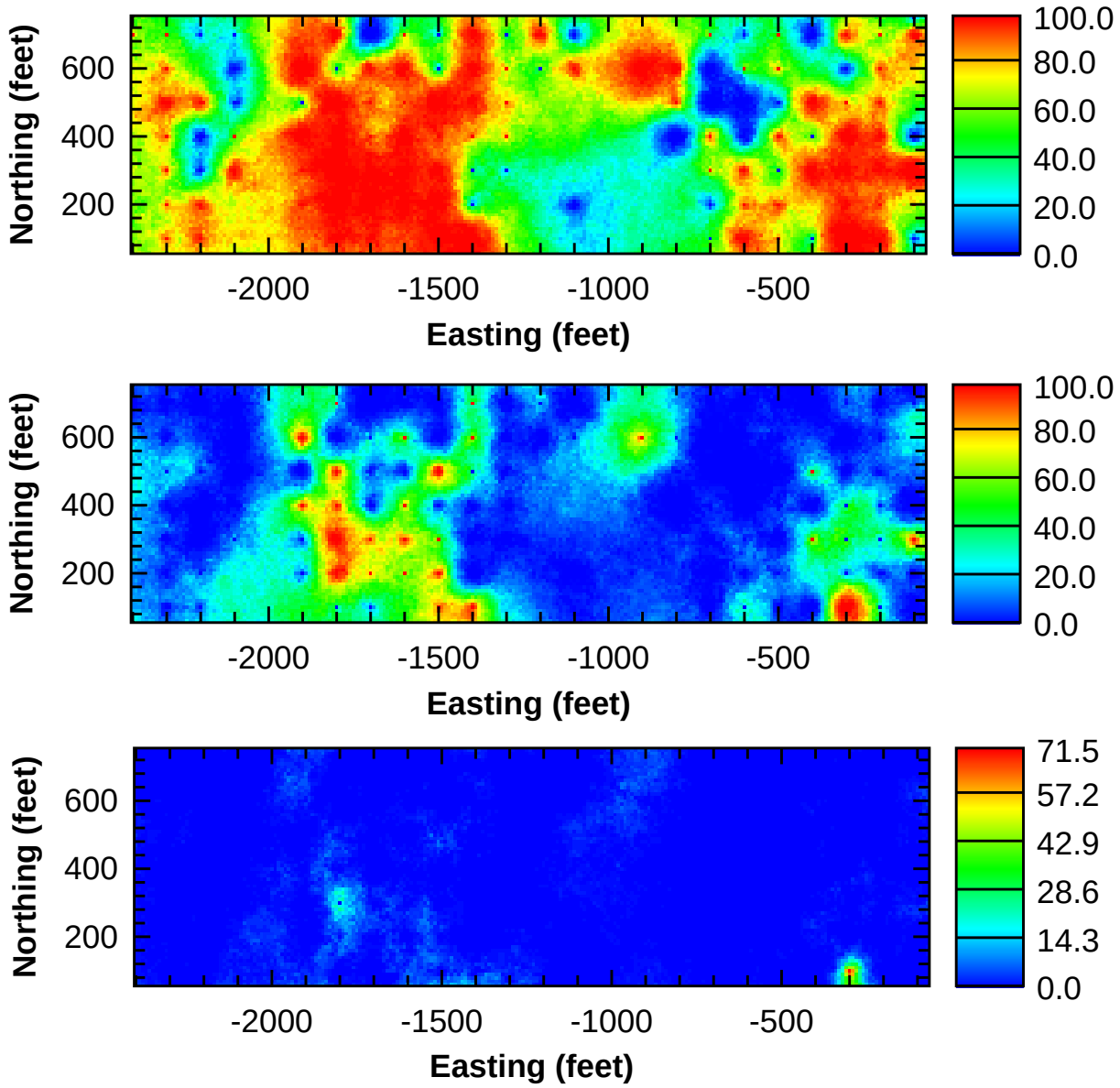

Figure 16. Probability of exceeding the action level (in percent) based on 100 realizations created with the continuous deposition conceptual model. The images correspond to action levels of 10 (top), 25 (center) and 50 (bottom) pCi/g.

ure 19. The parabolic function shown diagrammatically in Figure 19 is used in the WSD technique to determine the optimal additional locations in this study. The WSD technique could also be accomplished with other types of functions (ie., linear, exponential).

The third, decision-based technique employed in this study is the "reference uncertainty" (RU) technique, written as:

$$R(x) = \frac{C_{0.75} - C_{0.25}}{1 + \left| C_{0.5} - C_{\dot{A}\dot{L}} \right|}.$$

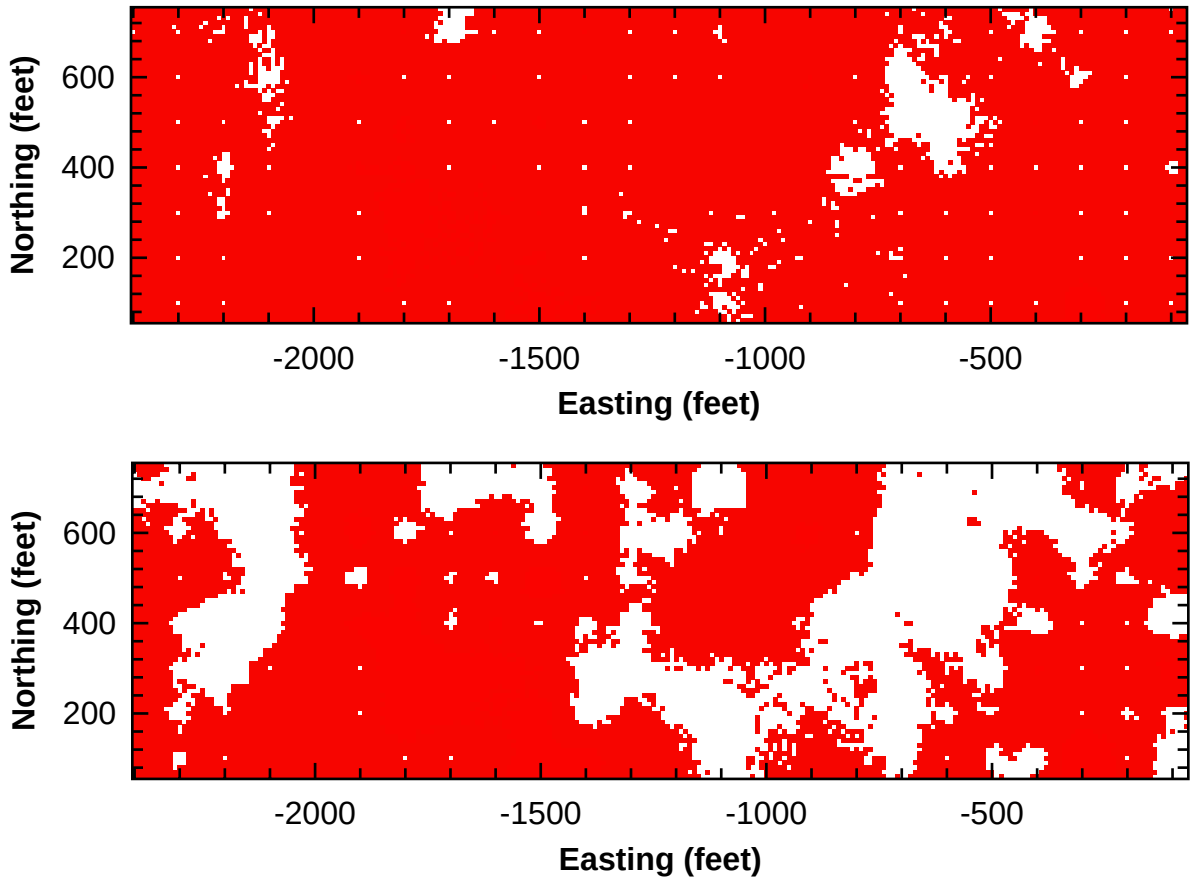

Figure 17. Two example remediation maps for the random depositional model (upper image) and the continuous deposition model (lower image). The red areas require remediation at an action level of 25 pCi/g and an acceptable pfail of 0.05.

The reference uncertainty at location *x*, *R(x)*, is the interquartile range ($C_{0.75}$ - $C_{0.25}$) of all the concentrations simulated at location *x*, divided by one plus the absolute value of the difference between the median concentration $C_{0.5}$ and the action level concentration $C_{A.L.}$ Similar to the weighted standard deviation technique, the reference uncertainty value will increase both as the variability of the simulated concentrations at a location increases and as the difference between the simulated values and the action level decreases. The idea behind a reference uncertainty is presented in Kyriakidis (1996), where it was used to determine the remediation panels with the greatest uncertainty of exceeding the action level. Here, the reference uncertainty is used to evaluate the uncertainty about the action level of potential sample locations across the simulated area. These three techniques all incorporate the action level into determining the locations of the additional samples. For comparison purposes, the conventional (unweighted) simulation standard deviation (SD) is also examined as a means of locating additional samples. The calculations are performed for the 25 pCi/g action level only.

All of the techniques discussed for determining the optimal locations of additional samples produce a continuous distribution of values from 1 to N, where N is equal to the number of elements in the simulation. The locations within the simulation can then be ranked from the maxi-

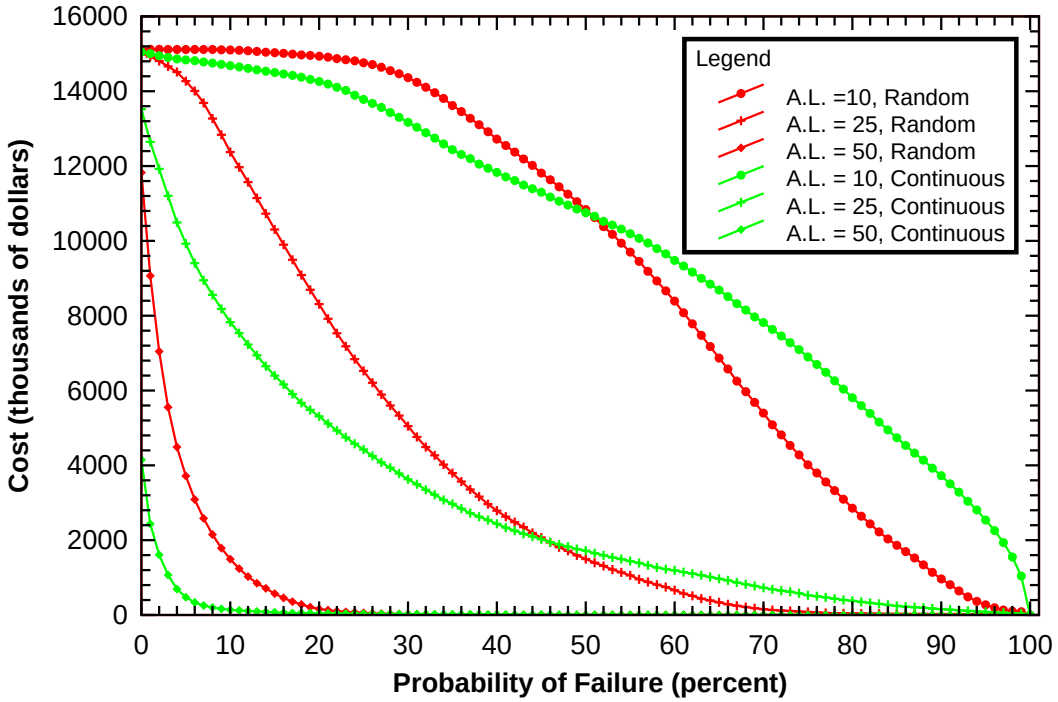

Figure 18. Cost curves for Release Block D. These curves are calculated from the probability maps in Figures 15 and 16. It is assumed that the distribution of concentration in the samples applies to 10x10x0.5 foot remediation units and that the remediation cost is $500/yd^3.

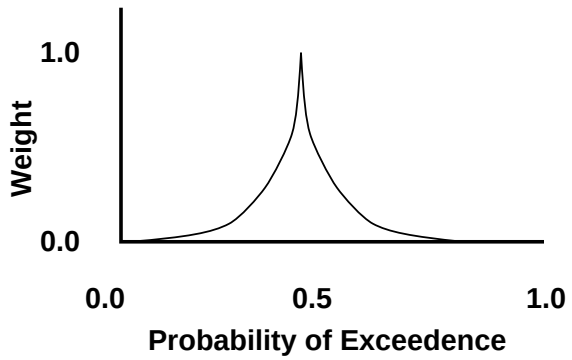

Figure 19. Conceptualization of the parabolic weighting function used in the weighted varaince technique for locating additional samples.

mum (1) to the minimum (N) value of the uncertainty measure (i.e., proximity to the median probability of failure, highest weighted variance, and highest reference uncertainty). It is still necessary to determine the number of additional samples to be taken in the follow-up sampling campaign. This number may be set by budgetary constraints, or by some other means, but it will

almost always be between 1 and the number of samples in the initial sampling campaign. Results reported by Englund and Heravi (1994) suggest that the best results are obtained when 75 to 80 percent of the total values acquired at the site are in the initial sampling. Following this convention and considering the initial 127 data locations to represent 77 percent of the eventual total data, another 39 samples should be acquired.

The results of determining the optimum locations for the 39 follow-up samples for each of the four techniques considered are shown in Figures 20 and 21 for the random and continuous deposition models respectively (refer to the probability maps for the 25pCi/g action level in Figures 15 and 16 to gain a better understanding of the follow-up sampling locations in Figures 19 and 20). Although not calculated here, the areas of maximum kriging variance occur in the locations without any nearby data. However, the large gap in the center of the sampling grid between easting coordinates -900 and -1200 feet has only a few locations targeted for a further sampling by the various techniques. The reason additional samples are not deemed necessary in this region is because the data points surrounding the gap in the grid are all associated with relatively low concentrations. This result highlights the need for considering the data values and the action level in planning any follow-up sampling campaign.

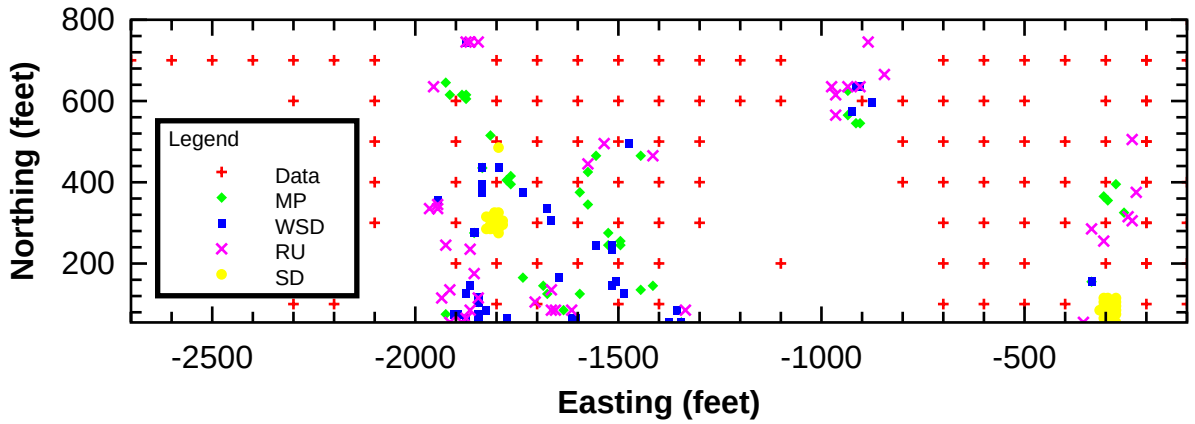

Figure 20. Locations of 39 follow-up samples as determined by each of the four techniques: median probability of failure (MP), weighted standard deviation (WSD), reference uncertatinty (RU) and simulation standard deviation (SD). The results are for the random deposition model. The existing data are shown for reference.

The three techniques for determining the locations of follow-up samples that consider the action level (MP, WSD and RU) provide relatively similar locations for these follow-up samples. In general these three techniques target the areas of greatest uncertainty with respect to the action level. These areas correspond to the median probability of exceedence areas (green colored areas of Figures 15 and 16). Understanding the subtle differences between the techniques and developing a technique that will use the best features of all techniques is a current research topic at SNL. The simulation standard deviation (SD) technique places all additional samples in two small areas. The SD technique does not consider the action level, but only areas of high variability. If the variability at a location is high, but all values within the distribution are still above, or below, the action level, then locating additional samples at that location is not effective in defining the

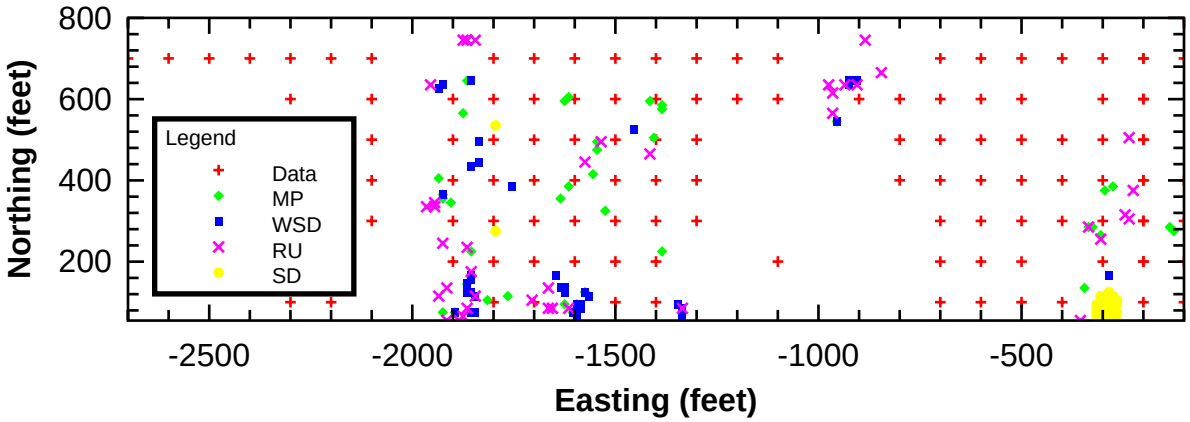

Figure 21. Locations of 39 follow-up samples as determined by each of the four techniques: median probability of failure (MP), weighted standard deviation (WSD), reference uncertatinty (RU) and simulation standard deviation (SD). The results are for the continuous deposition model. The existing data are shown for reference.

extent of contamination. An example of this situation is the area along the south edge of the domain at an easting coordinate of -300. The probability maps (Figures 15 and 16) show the probability of exceeding 25pCi/g to be near 100 percent at this location, yet the variability is still high and the SD technique suggests further sampling in this area.

It is noted that the follow-up locations for each technique are determined strictly on the rank of each uncertainty measure at a location; the techniques do not consider the proximity of another potential follow-up sample when determining the location. If the locations of other potential follow-up samples are considered in the ranking process, then the locations with the highest ranks will be more evenly spread across the domain. As an example, if three locations with the three highest ranks for locating additional samples are all next to each other, then obtaining a sample at the location with the highest rank will also provide information on the other two potential sample locations. This additional information will most likely decrease the uncertainty at those locations and lower the rank of each location for taking another sample.

Summary

Geostatistical simulation provides a useful tool for examining the uncertainty inherent in remediation planning and in further sampling. Uncertainties in remediation and sampling plans and the costs associated with them are due to uncertainty in the spatial distribution of the contaminant across the site. Knowledge of the conceptual model of the contaminant deposition is essential to completing an accurate sampling and remediation plan at a site. Large differences in the estimates of remediation costs are noted at Release Block D for the random and continuous conceptual models of deposition. Work with exhaustive data sets (e.g., Englund and Heravi, 1994) has shown that techniques for locating follow-up samples that incorporate the action level are superior to other techniques (kriging variance, simulation variance) that only measure variability of the concentration at a location. The comparison of techniques done on Release Block D sup-

port this conclusion; however, it is necessary to collect the follow-up samples within Release Block D to actually determine the improvement in remediation efficiency.

References

Barnes, R.J., 1989, Sample Design for Geologic Site Characterization, *Geostatistics, Vol. 2*, M. Armstrong (ed.), Kluwer Academic Publishers, Dordrecht, pp. 809-822.

Bear, J., 1979, *Hydraulics of Groundwate*r, McGraw Hill, Mew York, 569 pp.

Burgess, T.M., R. Webster and A.B. McBratney, 1981, Optimal Interpolation and Isarithmic Mapping of Soil Properties. IV Sampling Strategy, *Journal of Soil Science*, Vol. 32, pp 643-659.

Deutsch, C.V. and A.G. Journel, 1992, *GSLIB: Geostatistical Software Library and User's Guide*, Oxford University Press, New York, 340 pp.

EG&G Mound Applied Technologies, 1996, Removal Action Design, Operable Unit 4, Miami-Erie Canal, 100% Draft Final Design Document, April

EG&G Mound Applied Technologies, 1995, Operable Unit 5, Operational Area Phase 1 Investigation, Non-AOC Field Report (March Draft), Volume 2, Appendix D

Englund, E.J. and N. Heravi, 1993, Conditional Simulation: Practical Application for Sampling Design Optimization, in: A. Soares (ed.) *Geostatistics Troia '92,* Kluwer Academic Publishers, Dordrecht, pp. 613-624.

Englund, E.J. and N. Heravi, 1994, Multi-Phase Sampling for Soil Remediation, *Environmental and Ecological Statistics*, Vol. 1, No. 4, pp. 247-263.

Isaaks, E.H. and R.M. Srivastava, 1989, An Introduction to Applied Geostatistics, Oxford University Press, New York, 561 pp.

Knowlton, R.G., D.M. Peterson, D.D.Walker, B. Rutherford, J.E. White and B. Bullard, 1995, (unpublished) OPTMAS: Optimization Program to Minimize Analytical Sampling. Theory., Sandia National Laboratories, Albuquerque, NM, 42 pp.

Kyriakidis, P.C., (preprint), Selecting Soils for Remediation in Contaminated Soils Via Stochastic Imaging, in: *Proceedings of the Fifth International Geostatistics Congress*, Kluwer Academic Publishers, Spetember 22-27, Wollongong, Australia

Olea, R.A., 1984, Sampling Design Optimization for Spatial Functions, *Mathematical Geology,* Vol. 16, No. 4, pp. 369-392.

Rautman, C.A., P.G. Kaplan, M.A. McGraw, J.D. Istok and J.M. Sigda, 1994, Probability Mapping of Contaminants, in: *Cost Efficient Acquisition and Utilization of Data in the Management of Hazardous Waste Sites, Proceedings of the International Specialty Conference, March 23-25,* Air and Waste Management Association, Pittsburgh, PA, pp. 353-361.

Walpole, R.E. and R.H. Myers, 1989, *Probability and Statistics for Engineers and Scientists, Fourth Edition*, MacMillan Publishing Company, 765 pp.

Wingle, W.L., E.P. Poeter, S.A. McKenna and J.S. Brown, 1995, UNCERT: A Geostatistical Uncertainty Analysis Package Applied to Groundwater Flow and Contaminant Transport Modeling, User's Guide, Colorado School of Mines, Golden, Colorado.